A First-Principles Description of Liquid BeF_2 and Its Mixtures with LiF: 1. Potential Development and Pure BeF_2

Robert J. Heaton, Richard Brookes, Paul A. Madden,* Mathieu Salanne, Christian Simon, and Pierre Turq

Chemistry Department, University of Edinburgh, Edinburgh EH9 3JJ, UK, and Université Pierre et Marie Curie-Paris 6, CNRS, ESPCI, UMR 7612, Laboratoire LI2C, Case Courrier 51, 4 Place Jussieu, 75252 Paris Cedex 05, France

Received: February 16, 2006

The construction of an interaction potential for BeF_2 and its mixtures with LiF on a purely first-principles basis is described. The quality of the representation of the forces on the ions obtained from ab initio electronic structure calculations by various potentials, which include many-body interaction effects to different extents, are considered. The predictions of the properties of pure BeF_2 obtained in simulations with a polarizable potential are then compared with experimental values. In the subsequent paper, a more extensive comparison of the predicted properties of LiF−BeF_2 mixtures with experiment is considered.

I. Introduction

The development of accurate models of ionic melts is an important challenge in the field of computer simulation of material properties. Apart from the intrinsic interest in these systems, which may exhibit nontrivial structures, strong glass-forming tendencies, and liquid−liquid phase transitions inter alia, melts are involved in numerous current and proposed technologies. These often involve extreme temperatures and dangerous or corrosive materials so that the ability to predict physical properties over a wide range of conditions is valuable. Also, the ability to examine in simulations the microscopic events in processes such as corrosion and electrodeposition may lead to an improved understanding and better control.

These motivating factors are well represented by the target of our present study: BeF_2 and its mixtures with LiF. BeF_2 is a close structural analogue of SiO_2, exhibiting the same set of crystal structures[1] and atomic order in the glass.[2] At ambient pressures, liquid BeF_2 forms a tetrahedrally coordinated network that exhibits a "strong" glass transition and is believed to exhibit a liquid−liquid-phase transition.[3] These transitions occur at much lower temperatures than for SiO_2 so that there is a prospect of detailed diffraction studies in the régime of the transitions. When BeF_2 is combined with LiF, the network is broken down to some degree in a similar way that that of SiO_2 is broken up by the addition of alkali oxides. This prompts a very substantial reduction in the viscosity,[4] although this occurs in a far from monotonic way with composition, and it is a significant challenge to see if this can be linked to the changing character of the network. At the composition 53.1% in BeF_2, the mixture forms a eutectic at a temperature of 637 K. In part because of the relatively low temperature and viscosity of this liquid but also because of the very good nuclear properties of its constituents (moderating ratio, short- and long-lived activation), it has great potential in a variety of applications related to nuclear industries. The LiF−BeF_2 mixture becomes the material of choice as a solvent for actinide ions in the molten-salt reactor[5] and as a heat exchanger or blanket material in proposed breeder and fusion reactors.[6] Because of these potential applications, an enormous amount of experimental work has been done on LiF−BeF_2[7] and it is by far the best-characterized fluoride melt. For this reason, it is the ideal testing ground for evaluating the first-principles approach to construction of interaction potentials for fluorides, which we describe below.

It is now well-recognized that the potentials needed to model interactions in ionic materials must embrace the concept that ions in the condensed phase are profoundly different from their gas-phase counterparts.[8] In an ideal world, simulations would avoid the introduction of model potentials and adopt an ab initio MD approach, but unfortunately, these methods cannot yet access the time scales necessary to study these viscous materials reliably. In the most straightforward case, such as a single phase of an alkali halide, the concept can be realized through a simple pair potential,[8,9] viewed as the interaction between condensed-phase ions. However, to obtain transferable potentials, some explicit representation of many-body effects is necessary. It has recently been demonstrated, in work on polyvalent metal *chlorides* that the most important corrections involve polarization effects.[10] Polarizable potentials were refined against structural information from diffraction experiments on pure melts and shown to *predict* accurate values for transport coefficients[11] and vibrational spectra for the pure materials and their mixtures with alkali chlorides,[12] among other properties. Similar potentials should also describe the fluorides, but because of the difficulty of performing diffraction experiments on these highly corrosive materials at comparatively high temperatures, there is no structural information on which to refine the potentials and select parameters. Consequently, we need to adapt an ab initio "force-fitting" procedure, previously applied to oxides,[13,14] in order to construct a set of fluoride potentials. Because of the unusually large amount of experimental information available for LiF−BeF_2, it is a natural first application.

There have been a number of previous simulation studies of BeF_2 using effective ionic pair potentials. There is a brief report of early work by Rahman et al[15] that included simulations of LiF−BeF_2 mixtures. Brawer and Weber[16] made an extensive study of the role of coordination defects on ion dynamics in

* Corresponding author. E-mail: paul.madden@ed.ac.uk.

10.1021/jp061000+ CCC: $33.50
Published on Web 05/24/2006

the glass. Recently, Angell and co-workers[17] have conducted long simulations to examine the possibility of observing liquid−liquid-phase transitions in the system. Although these simulations describe the average structure of liquid BeF_2 as a tetrahedrally coordinated network liquid, in qualitative accord with experiment, they have not been compared with experimental measurements at the quantitative level. Wright and co-workers[2] did compare their neutron structure factor for the glass with that calculated from quenched structures from Brawer's simulations and concluded that the simple pair potentials overestimated the flexibility of the first coordination shell and failed to give the correct Be−F−Be bond-angle distribution. As has been discussed extensively elsewhere,[18] anion polarization effects have an important effect in controlling the bond-angle distribution in ionic materials and we would expect them to be the most important of the many-body effects to be included in our interaction model.

In the next section, we describe the application of the force-fitting procedure to BeF_2. We then compare results from simulations with the properties of the pure melt, including the equation of state, diffraction structure, diffusion coefficient, and infrared spectrum. These comparisons are included primarily to validate the potential, as there has been a good deal of previous simulation work on the pure material, often with pair potentials so that there is already a good microscopic understanding of most of its properties. For the solutions, on the other hand, pair potentials have been less successful because of inherent problems of transferability. In the following paper, we demonstrate quantitative agreement with the experimental information and provide insight into the process of network-breaking as the LiF is added.

II. Ab Iinitio Potentials for BeF_2 and its Mixtures with LiF

Detailed descriptions of the "force-fitting" procedure, as applied to oxides, have been give recently.[13,19] Here, we will focus on features specific to the fluoride systems of interest here.

In the force-fitting process, we set up several representative condensed-phase configurations for BeF_2, each containing roughly 100 ions in periodic boundary conditions, by using an approximate interaction potential and then performing ab initio electronic structure calculations using the planewave DFT CASTEP[20] code on them. These are analyzed to give the components of the force and the dipole and quadrupole on each ion in each configuration and the components of the stress tensor for the whole cell. We then fit the potential by varying the parameters in the potential to minimize the difference between the ab initio forces, etc., and those predicted by the potential model for the given atomic arrangement.

For BeF_2, the configurations were derived from high-temperature MD simulations of the α-quartz (four-coordinate), high-cristobalite (four-coordinate), stishovite (six-coordinate),[1] and liquid phases of BeF_2. The atoms in these configurations sampled a wide range of thermally distorted environments, and the aim was that, by using a sufficiently large and varied set of such configurations, a transferable potential would be obtained. The ab initio DFT calculations used nonlocal ultrasoft pseudopotentials[20] for all ions (four electrons for Be and seven for F), together with the PW91[21] GGA exchange-correlation functional, and a kinetic energy cutoff of 580 eV to ensure a high degree of convergence of the forces. The finite basis set correction to the stress tensor was estimated by performing calculations at three different values of the kinetic energy cutoff. The multipole moments of the individual ions were then calculated by using the technique described in Aguado et al.,[13] where the moments of the charge density around each ion are obtained from a maximally localized Wannier function transformation from the Kohn−Sham orbitals output from the electronic structure calculation. In BeF_2, the Wannier functions localize close to the nuclear positions in a way consistent with an ionic picture of the interactions (i.e., Be^{2+}, F^-).

First, we determined the polarization parameters in the potential by fitting the multipoles predicted by the model to the ab initio calculated ones. For the dipole-polarizable model, for example, this was done by minimizing the objective function

$$A_{\mathrm{P}}(\{\chi_{\mathrm{P}}\}) = \frac{1}{2}\sum_{i,A}\frac{\sum_{\alpha}|\mu_{i,\alpha}^{A}(\{\chi_{\mathrm{P}}\}) - \mu_{i,\alpha}^{A,\mathrm{ai}}|^2}{\sum_{\alpha}|\mu_{i,\alpha}^{A,\mathrm{ai}}|^2} \qquad (2.1)$$

and allowing the set of parameters $\{\chi_{\mathrm{P}}\}$ to vary. In this expression, the index i runs over atoms, and the index $\alpha = x, y, z$ runs over the three dipole components. The sum over A represents the sum over all atomic configurations included in the fit. To optimize the objective function, a nongradient simplex method was used.

The set of forces and stresses obtained directly from CASTEP were then used to minimize the objective function

$$A_{\mathrm{F}}(\{\chi\}) = \frac{1}{2}\sum_{i,A}\frac{\sum_{\alpha}|F_{i,\alpha}^{A}(\{\chi\}) - F_{i,\alpha}^{A,\mathrm{ai}}|^2}{\sum_{\alpha}|F_{i,\alpha}^{A,\mathrm{ai}}|^2} + \frac{1}{2}\sum_{A}\frac{\sum_{j,k}|S_{jk}^{A}(\{\chi\}) - S_{jk}^{A,\mathrm{ai}}|^2}{\sum_{j,k}|S_{jk}^{A,\mathrm{ai}}|^2} \qquad (2.2)$$

as a function of the set $\{\chi\}$ of short-range potential parameters while holding the polarization parameters fixed. $F_{i,\alpha}^{A,\mathrm{ai}}$ and $S_{jk}^{A,\mathrm{ai}}$ refer to the α-component of the ab initio force on ion i and an element of the stress tensor in the ab initio calculation of configuration A and $F_{i,\alpha}^{A}(\{\chi\})$ and $S_{jk}^{A}(\{\chi\})$ to those calculated from the model with parameters $\{\chi\}$ in the same ionic configuration. The quality of these fits is illustrated in Figure 1 for a full "aspherical ion" potential (AIM),[14] which allows for induced dipoles and quadrupoles as well as deformations of the shapes of the anions of dipolar and quadrupolar symmetry.[22] The abcissa in these plots represent the index of an ion in a configuration of the structure indicated and the ordinate gives values for the chosen quantity (force, dipole, etc.) for that ion, with the point giving the ab initio value and the line the value predicted by the fitted potential. The first two-thirds of the ions in any configuration are anions, and the remainder are cations. Note that the ab initio cation multipoles are much smaller than the anion ones, which justifies a model in which cation polarization is ignored. Uniformly good fits across the range of configurations is indicated and particularly for the forces and dipoles. The predictions of the quadrupole moments are less good, especially for the quartz and crystobalite configurations. This could be improved by allowing the quadrupole polarizability to be dependent on the coordination number. The values of the objective functions were $A_{\mathrm{P}} = 0.0897$ and $A_{\mathrm{F}} = 0.0832$, which we regard as indicating very good fits.

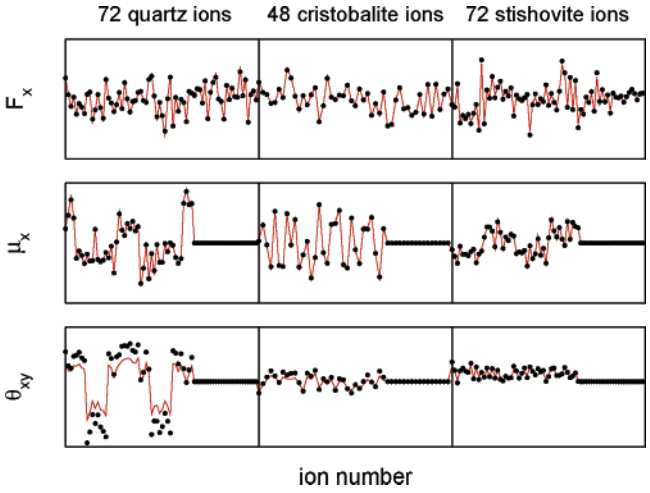

Figure 1. The quality of the fits of the forces and dipole moments on the ions to those obtained from the ab initio calculations is shown for three different configurations. The solid lines show the predictions of a full "AIM" potential,[14] and the points the results from the ab initio calculations. For each configuration, the cation values are shown second, and the multipoles much smaller than those of the anions.

Because the immediate intention was to run long simulations on large cells of these viscous materials, we examined whether it would be possible to obtain a simpler model, suitable for the liquid phase, which, as we will see, has similar local structures to the tetrahedrally coordinated crystals. In this potential, we dispense with the particularly time-consuming elements of the AIM potential dealing with ion shape deformation, which were introduced to allow the potential to be transferable across a wide range of coordination structures[22] and retain anion dipole polarization as the only many-body effect (a "polarizable ion model" (PIM)). Such potentials had, after all, been shown to work well for the chlorides.[10] The full AIM potential will be used in future work on the effect of pressure on the glass.

Repeating the fit for a PIM potential to the same set of ab initio data gives uniformly good fits across the range of *four*-coordinate configurations sampled (including the liquid), however, the fit was not as good in the six-coordinate stishovite structure. The value of objective functions were $A_P = 0.0140$ (the smaller value with respect to the full aim fit being due to the omission of the quadrupoles from the polarization model) and $A_F = 0.137$, the poorer fit for the stishovite ions leading to the higher value of A_F than the AIM fit above. If we omit the stishovite configurations so that only tetrahedrally coordinated structure are involved, and recalculate the values of A_P and A_F, we obtain $A_P = 0.0138$ and $A_F = 0.0839$. It would seem that the simpler potential should be adequate for our immediate needs.

Finally, because the object of the exercise is to simulate LiF−BeF_2 *mixtures*, we attempted to fit a PIM model to BeF_2 and LiF configurations *simultaneously* to obtain a compromise potential to describe the F−F interactions in both materials and, it is hoped, their mixtures. It should be noted that the existence of a good compromise potential is by no means obvious. In the tetrahedrally coordinated phases of pure BeF_2, the coordination number of the F^- ions is two, whereas in molten LiF, it is close to four and in the crystal to six, so that, on general grounds, we should expect the fluoride ions themselves to be appreciably different in these phases. We previously described a study of LiF itself.[19] The consequence of this exercise is a potential for which we specify all parameters in the appendix. When applied to the tetrahedral BeF_2 configurations alone (without further optimization), we obtain objective function values of $A_P = 0.0149$ and $A_F = 0.0519$, which indicates that this potential is not substantially worse than could be obtained by fitting a PIM model to the BeF_2 data alone. This is the potential we have used in the liquid-state studies described below.

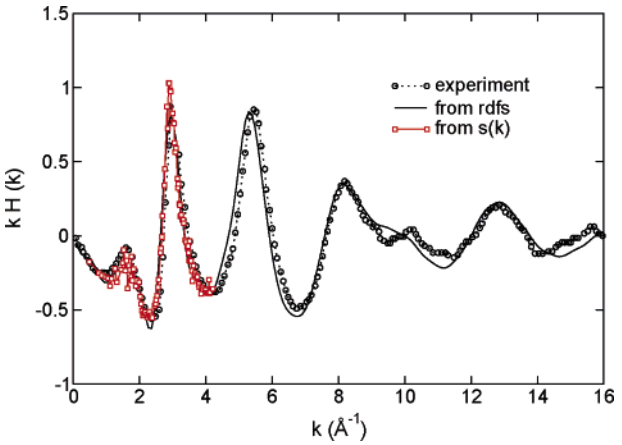

Figure 2. The reduced intensity functions for the dipolar ion model at 1300 K compared to that measured experimentally at 973 K. In the figure, the black circles are the experimental data points,[26] the full line uses structure factors obtained from eq 3.1, while the red line and point those from eq 3.2.

One final remark concerns the way in which the dispersion parameters in the interaction potential have been handled; dispersion is described by pair potentials in the usual way. As is well-known, dispersion terms are not reliably described in DFT calculations[23] so that ab initio calculations do not provide a good way of optimizing them. Consequently, we have introduced suitable values for the dispersion parameters, which only significantly affect the F−F interactions in this system and are obtained from previous studies of CaF_2[24] and held them fixed throughout the fitting process.

III. Predicted Properties of Pure BeF_2

To test the BeF_2 potential, we made a set of long MD runs (up to 1 million steps) at a series of temperatures, keeping the density fixed at the experimental value at 973 K (1.96 g cm^{-3}). Several experiments have been made at this temperature, so it provides a useful reference point, although, as we will see, the simulations cannot be properly equilibrated at temperatures below about 1250 K because of the slow dynamics associated with the proximity to the glass transition. The methods employed in the MD simulations have been described in earlier papers.[25] In almost all runs, we used 432 ions. Simulations were carried out at temperatures ranging from 1300 to 2400 K. The systems were set up with a velocity rescale, using the ionic configuration generated in a previous run at a higher temperature, and were then run-on for a length of time greater than 5 structural relaxation times at the selected temperature, each over 1 ns, to achieve equilibration. The runs were then continued without further velocity rescaling, and the trajectories were used for the analysis which follows.

The simulated systems show an atomic structure that can be described as a near-perfect tetrahedral network. At the lower temperatures, just 1% of the Be^{2+} ions have a coordination number other than 4, and all except a similar percentage of F^- ions are forming "bonds" to just two Be^{2+} ions. At 2400 K, there are substantially more broken bonds, with 24% of Be^{2+} ions exhibiting coordination numbers other than 4.

A. Structure and X-ray Diffraction. We calculated the X-ray-reduced intensity function from an MD simulation at 1300 K (Figure 2). This simulation was run for over 3 ns to allow

for equilibration, several structural relaxation times for the system at this temperature. A further 1 ns simulation was then used for data collection. The calculated data will be compared with experimental information obtained by Narten at 973 K,[26] but at the same density as the simulations.

To calculate the X-ray-reduced intensity function, we first calculated each partial static structure factor from the Fourier transform of the corresponding partial radial distribution according to

$$S_{\alpha\beta}(k) = \delta_{\alpha\beta}x_\alpha + x_\alpha x_\beta \rho \int_0^\infty 4\pi r^2 \frac{\sin(kr)}{kr}[g_{\alpha\beta}(r) - 1]\, dr \tag{3.1}$$

where ρ is the number density for all ions present and x_α is the mole fraction of species α. To circumvent problems with truncation errors in the Fourier transform, we also calculated partial structure factors by direct summation over the ionic positions

$$S_{\alpha\beta}(k) = \langle (N_\alpha N_\beta)^{-1/2} \sum_{i\epsilon\alpha} \sum_{j\epsilon\beta} e^{i\mathbf{k}.\mathbf{r}_{ij}} \rangle \tag{3.2}$$

where **k** is a wavevector commensurate with the periodic boundary conditions. This method gives a more reliable structure factor at low *k*. The total X-ray structure factor can then be cast in terms of the partial structure factors as

$$S_{X-ray}(k) = f_1(k)^2 S_{11}(k) + 2f_1(k)f_2(k)S_{12}(k) + f_2(k)^2 S_{22}(k) \tag{3.3}$$

Form factors, f_α, were obtained from the *International Tables for Crystallography*.[27]

For BeF_2, the experimental X-ray data[26] is reported in the form of the reduced intensity function, $k{\cdot}H(k)$, where

$$k{\cdot}H(k) = k\frac{S_{X-ray}(k) - \sum_{\alpha=1}^{2} x_\alpha f_\alpha(k)^2}{(\sum_{\alpha=1}^{2} x_\alpha f_\alpha(k))^2} \tag{3.4}$$

In the figure, the calculated data points coming from eq 3.2 are indicated by squares, whereas those from 3.1 are indicated by the full line. Although the former are affected by statistical fluctuations, this method is useful for the low-*k* region and for reproducing the shape of the "prepeak" in the diffraction data at $k \sim 1.8$ Å^{-1}. The comparison indicates a very good agreement between the experimental data and the simulation, the only exceptions being in the region around 10 Å, where the experimental data are more sharply peaked than the simulation, and in a small shift in the peak at 5.7 Å^{-1}. It is possible that the discrepancies are due to the fact that the simulation temperature is higher, but we were unable to check this because we could not equilibrate at the lower temperature. The agreement with the diffraction data is much better than obtained previously for the glass with an effective pair potential.[2]

In Figure 3, the bond-angle distributions for the F−Be−F and Be−F−Be bonds in the simulation at 1300 K are shown. The former is peaked sharply about the tetrahedral angle, while the latter is peaked around 137°. This nontrivial bond angle arises in our simulations as a consequence of the fluoride ion dipole polarization effects.[18] Wright et al.[2] deduced a most probable bond-angle of 143° from their analysis of the neutron diffraction by the glass at room temperature.

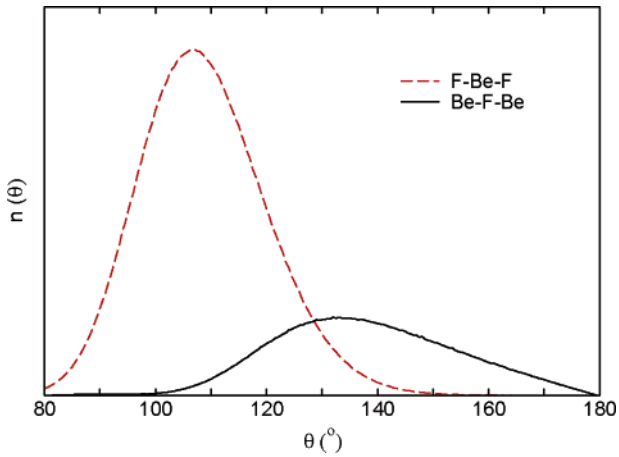

Figure 3. Bond-angle distributions from the simulation of BeF_2 at 1300 K.

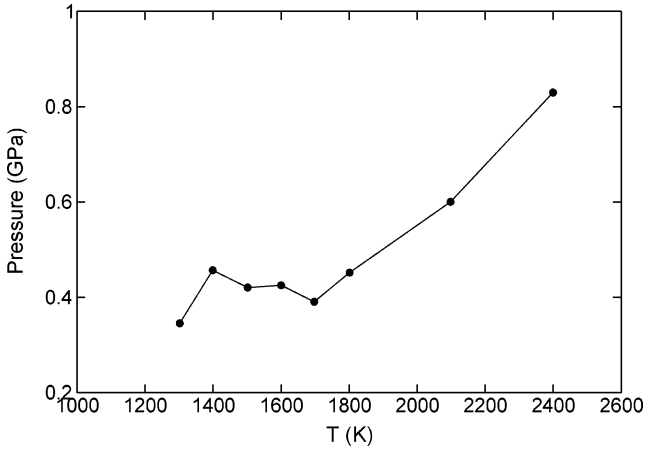

Figure 4. Variation of pressure with temperature at the fixed density $\rho = 1.96$ g cm^{-3}. The minimum of the isochore gives the temperature at which the density passes through a maximum value.

B. Equation of State. We have undertaken a limited examination of the equation of state by calculating the pressure generated by the system at each of the temperatures simulated and the chosen density. A more extensive analysis was carried out by Hemmati et al.[17] with their TRIM pair potential in order to examine the possibility of liquid−liquid-phase transitions in this system. In Figure 4, we show the variation of pressure with temperature for our simulations. The pressures observed at the 973 K laboratory density are much lower than those using the TRIM potential, and from the lower temperature points, it looks as if the pressure will continue to decrease as temperature decreases to give a pressure close to zero at 973 K as appropriate for this density. A notable feature of the data is the nonmonotonic behavior of the pressure with temperature around 1700 K; as Hemmati et al. have explained,[17] this may indicate the presence of a liquid−liquid-phase transition in BeF_2 analogous to that discussed for other tetrahedrally coordinated liquids such as Si, H_2O, and SiO_2[3]. From the relation

$$(P/T)_V = \alpha/\kappa_T \tag{3.5}$$

where α is the thermal expansivity and κ_T is the isothermal compressibility, it can be seen that the pressure will exhibit a minimum if $\alpha = 0$, that is, if the density passes through a maximum. If there is a second extremum in *P* at an even lower temperature, then this will correspond to a second change in the sign of the expansion coefficient and will indicate the presence of a density minimum. The results for the TRIM

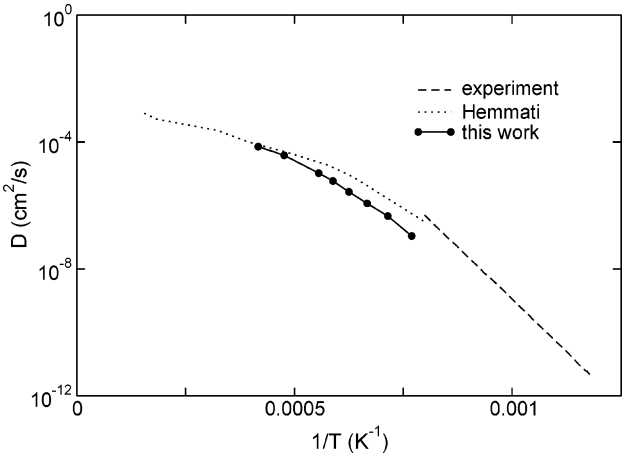

Figure 5. Arrhenius plot of the F^- ion diffusion coefficients in BeF_2 compared with those scaled from viscosity data using the Eyring equation and the simulation results of Hemmati et al.

potential[17] show a minimum in *P*, for each of the volumes simulated, close to 2000 K, and possibly a maximum in *P* at the lower temperature of 1250 K, although this extremum is not clear as, at these temperatures, the simulations are difficult to equilibrate. From the figure, we can see that, for our potential, there is a minimum in the isochore at 1700 K. In addition, we may also be seeing a maximum in the isochore at a lower temperature close to 1400 K, although it should be noted that it is difficult to equilibrate the system at lower temperatures due to the slow dynamics and, therefore, to make the maximum evident by performing reliable calculations at 1200 K and lower.

C. Diffusion. We calculated the diffusion coefficients of the anions and cations from the mean-squared displacements by using the Einstein relation. Although the diffusion coefficents have not been measured directly for BeF_2, there have been measurements of the viscosity made between ~600 and 1200 K, and Hemmati et al.[17] suggested using them to estimate diffusion coefficients by using the Eyring equation, which seems to provide the best account of viscosity/diffusivity relations in these network liquids. The Eyring equation is

$$D_i = \frac{k_B T}{\eta \lambda_i} \tag{3.6}$$

where η is the viscosity and λ_i is the jump distance, taken in previous work to be the diameter of the fluoride anion. In Figure 5, we show the F^- ion diffusion coefficients obtained from these simulations and compare our results to those of Hemmati et al. with the TRIM potential and to the diffusion coefficients scaled from the viscosity measurements. The simulation values of diffusivity are close to those of Hemmati et al., and although they do not join the experimental "diffusivities" smoothly, the gradient of the curve obtained from our simulations seems to approach that of the expermental curve at the highest temperatures measured. As the Erying equation requires a choice of jump length, (λ_i, above) the vertical position of the experimental curves in Figure 4 would shift as the estimate of the jump length is altered. At higher temperature, we see the same curvature in the Arrhenius plot of the diffusion coefficients as was noted in the simulations of Hemmati et al. These data suggest again that the anomalous behavior of the viscosity of liquid BeF_2, relative to other liquids in the strong/fragile classification, will be resolved if the viscosity is obtained at higher temperatures and that it will curve over suddenly and join the other liquids in the approach to a common high-temperature limit. This mass transport behavior seen in Figure 4 has been described as a crossover from high-temperature fragile to low-temperature strong liquid behavior and is similar to the high temperature behavior observed in simulation studies of SiO_2[28] using various potentials. It has been suggested that this crossover may be related to the liquid−liquid-phase transition indicated by the equation of state. As we noted above, the Be^{2+} coordination number indicates that the tetrahedral network is almost perfect at 1300 K, the lowest temperature of our study, but that it has been strongly broken down at the highest temperature.

D. Infrared Spectrum. The infrared (and Raman) spectra of melts of polyvalent ions show discrete bands attributable to the vibrational motion of the local coordination complexes around the cations. A calculation of the infrared absorption spectrum of the melt, therefore, provides a significant additional test of the interaction model to those described above because it highlights the local Be−F interactions.[29] The IR absorption spectrum is caused by the polarization fluctuations associated with motion of the ionic charges. However, from a microscopic perspective, we can recognize the possibility that the dipoles *induced* in other ions may contribute to the polarization along with that associated with the charge currents themselves. The inclusion of polarization effects for the fluoride ions in our model may influence the predicted absorption spectrum in two ways. First, the interactions of the fluoride ion dipoles may alter the local structure of the network and the strength of the bonds so that shifts in the vibrational frequencies may occur. Second, the induced dipoles may themselves be responsible for absorption, as they too contribute to the total polarization fluctuations. The absorption coefficient in the presence of these extra moments is calculated from the imaginary part of the *total* dielectric function [$\alpha(\omega) \simeq \omega\, \mathscr{T}(\Xi(\omega))$], given by Caillol et al.[30] as

$$\Xi(\omega) - 1 = \frac{4\pi}{3Vk_BT}\Big\{\langle M(0)^2\rangle + i\omega\,\langle \mathbf{M}\cdot\mathbf{M}\rangle_\omega + 2\,\langle \mathbf{M}\cdot\mathbf{J}\rangle_\omega + \frac{i}{\omega}\langle \mathbf{J}\cdot\mathbf{J}\rangle_\omega\Big\} \tag{3.7}$$

where

$$\langle \mathbf{J}\cdot\mathbf{J}\rangle_\omega = \int_0^\infty \mathrm{d}t e^{i\omega t}\,\langle \mathbf{J}(t)\cdot\mathbf{J}(0)\rangle \tag{3.8}$$

$\mathbf{J}(t)$ is the charge current $\mathbf{J} = \sum_{i=1}^N q_i \mathbf{v}_i(t)$, and $\mathbf{M}$ is the total system *induced* dipole moment, $\boldsymbol{M}(t) = \sum_{i=1}^N \mu_i(t)$, obtained from the instantaneous induced dipoles predicted by the simulation potential. Here, ω is the frequency, V is the volume, k_B is Boltzmann's constant, and T is the temperature. These expressions have been used previously to examine infrared absorption in $ZnCl_2$[31] and SiO_2.[32]

Figure 6 shows the total absorption coefficient obtained in this way at 1300 K compared with that measured experimentally[33] for the glass. The experimental result is that for glassy BeF_2 at room temperature and has been scaled so that the peak at ~750 cm^{-1} is the same as that of the calculated total spectrum. Because the structure seen in the infrared spectrum above about 100 cm^{-1} is caused by the local vibrations within coordination complexes, we would not expect it to show a strong temperature dependence; the diffraction data[26] indicates very little change in structure in the first coordination shell between the liquid and glass. The calculated spectrum is in excellent agreement with that measured experimentally. There are two major peaks at 400 and 750 cm^{-1}, the same frequencies at which two peaks are observed experimentally;[33] we will discuss the

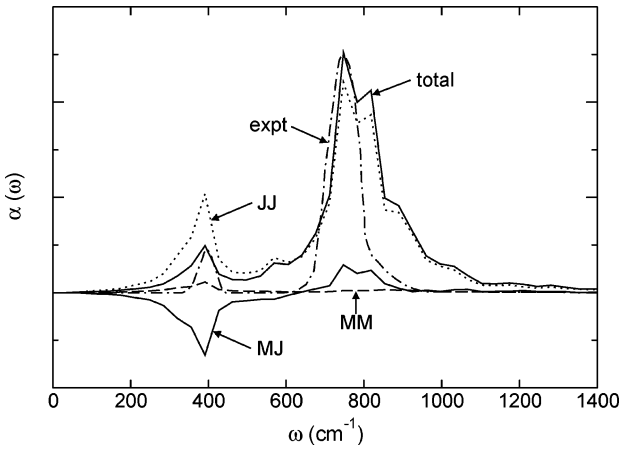

Figure 6. The total IR absorption spectrum (solid line) and its component parts, labeled JJ (short dashed line), MJ (solid line), and MM (long dashed line). The experimental spectrum is labeled expt (dash−dotted line).

characteristic motions associated with these features in the paper on LiF−BeF_2 which follows. Moreover, the ratio of the peak heights in the *total* calculated spectrum is seen to be almost identical to that in the experimental spectrum.

In Figure 6, we also show the separate contributions to the absorption associated with the $\langle \mathbf{M}\cdot\mathbf{M}\rangle_\omega$, $\langle \mathbf{M}\cdot\mathbf{J}\rangle_\omega$, and $\langle \mathbf{J}\cdot\mathbf{J}\rangle_\omega$ functions. This shows that there is a significant contribution to the spectrum from the interference between the induced dipole and permanent charge contributions to the total polarization contained in the $\langle \mathbf{M}\cdot\mathbf{J}\rangle_\omega$ cross-term. Including this term reduces the height of the 400 cm^{-1} peak and increases the height of the 750 cm $^{-1}$ one, producing a spectrum in very good agreement with experiment. A similar effect was noted in SiO_2,[32] and a microscopic explanation is given there.

IV. Conclusions

We have shown how an interaction potential for BeF_2 (and its mixtures with LiF) may be developed from first principles. We showed how a full "aspherical ion" (AIM) potential[14,22] could reproduce the ab initio calculated forces and multipoles for a set of configurations that spanned both tetrahedrally and octahedrally coordinated structures of BeF_2. This AIM potential will be used in future studies of pressure effects on glassy BeF_2. To facilitate simulations of the liquid and, in particular, its mixtures with LiF (to be described in the following paper), where long runs will be required, we also considered a simpler potential in which anion polarization was the only source of many-body effects. We showed that a good fit to the ab initio calculated properties of the tetrahedrally coordinated phases of BeF_2 could be obtained, even if we constrained the F−F interactions to be the same as in a similarly fitted potential for LiF[19] in order to allow simulations on LiF−BeF_2 mixtures. We then demonstrated the ability of this compromise potential to reproduce experimental data on pure BeF_2. We compared this with diffraction, diffusion, and infrared data, which probe structure and dynamics in the material on a wide range of length and time scales. We also showed that the potential predicted reasonable behavior for the equation of state for densities close to those of the liquid around melting. The ability to develop potentials of this quality without any reference to experimental information opens the way for predictive studies on other fluoride systems. In the following paper, we will show that the compromise potential allows an excellent description of the properties of LiF−BeF_2 mixtures.

TABLE 1: Potential Parameters

ion pair	B_{ij}	α_{ij}	C^6_{ij}	C^8_{ij}	b^6_{ij}	$b^8_{ij}ij$
F^-−F^-	181.84	2.267	15.0	150.0	1.9	1.9
Be^{2+}−F^-	41.72	2.254	0.0	0.0	1.0	1.0
Li^+−F^-	20.42	2.052	0.0	0.0	1.0	1.0
Be^{2+}−Be^{2+}	106.16	3.944	0.0	0.0	1.0	1.0
Li^+−Li^+	195.91	4.252	0.0	0.0	1.0	1.0
Be^{2+}−Li^+	151.72		0.0	0.0	1.0	1.0

Acknowledgment. P.A.M. is grateful to the Université Pierre et Marie Curie for his appointment as Professor Invité, which enabled this collaboration. The electronic structure calculations were performed on the HPC(x) computer at the Daresbury Laboratory through the UK Car−Parrinello Consortium.

Appendix: The Interaction Potential

The interaction potential actually used in the liquid-state simulations is a "polarizable ion model" and consists of a pair potential of Born−Mayer form together with an account of ionic polarization.[8] The pair potential is written

$$V(r_{ij}) = B^{ij}\, e^{-\alpha^{ij} r_{ij}} - f_{ij}^{\,6}(r_{ij})\frac{C_{ij}^{\,6}}{r_{ij}^{\,6}} - f_{ij}^{\,8}(r_{ij})\frac{C_{ij}^{\,8}}{r_{ij}^{\,8}} \quad \text{(A5.1)}$$

where C_{ij}^6 and C_{ij}^8 are the dispersion coefficients and $f_{ij}^{(n)}$ are dispersion damping functions[34] given by

$$f_{ij}^{(n)}(r_{ij}) = 1 - e^{-(b^n_{ij} r_{ij})} \sum_{k=0}^{n} \frac{(b_{ij}^{\,n} r_{ij})^k}{k!} \quad \text{(A.2)}$$

Values for all parameters necessary to simulate BeF_2 and its mixtures with LiF are given in Table 1. All the parameters are given in atomic units; the atomic unit of length is the Bohr radius (0.52918 Å) and of energy, the Hartree, 4.3597×10^{-18} J. The polarization parts of the potential include fluoride ion polarization only.[8,10] We used a fluoride ion polarizability of 7.09 Bohr^3 and applied a damping function

$$g_{ij}(r_{ij}) = 1 - c_{ij}\, e^{-(b_{ij} r_{ij})} \sum_{k=0}^{4} \frac{(b_{ij} r_{ij})^k}{k!} \quad \text{(A.3)}$$

to the interaction between the anion dipoles and the cation charges with $b_{\mathrm{FBe}} = 1.78$ au^{-1}, $b_{\mathrm{FLi}} = 1.81$ au^{-1}, $c_{\mathrm{FBe}} = 0.99$, and $c_{\mathrm{FLi}} = 1.40$

References and Notes

(1) Müller, U. *Inorganic Structural Chemistry*; Wiley: Chichester, 1993.
(2) Wright, A. C.; Clare, A. G.; Etherington, G. E.; Sinclair, R. N.; Brawer, S. A.; Weber, M. J. *J. Non-Cryst. Solids* **1989**, *111*, 139.
(3) Saika-Voivod, I.; Sciortino, F.; Poole, P. H. *Phys. Rev. E* **2004**, *69*, 041503.
(4) Cantor, S.; Ward, W. T.; Moynihan, C. T. *J. Chem. Phys.* **1969**, *50*, 2874.
(5) Haubenreich, P. N.; Engel, J. R. *Nucl. Appl. Technol.* **1970**, *8*, 118.
(6) Sahin, S.; Ubeyli, M. *Energy Convers. Manage.* **2005**, *46*, 3185.
(7) Robbins, G. D.; Braunstein, J. *Molten Salt Reactor Program, Semiannual Progress Report*, ORNL-4449, Oak Ridge National Laboratory, Oak Ridge, TN, 1969−1970.
(8) Madden, P. A.; Wilson, M. *Chem. Soc. Rev.* **1996**, *25*, 339.
(9) Tosi, M. P.; Price, D. L.; Saboungi, M.-L. *Annu. Rev. Phys. Chem.* **1973**, *44*, 173. Rovere, M.; Tosi, M. P. *Rep. Prog. Phys.* **1986**, *49*, 1001.
(10) Hutchinson, F.; Wilson, M.; Madden, P. A. *Mol. Phys.* **2001**, *99*, 811.
(11) Okamoto, Y.; Madden, P. A. *J. Nucl. Mater.* **2005**, *344*, 109.
(12) Glover, W. J.; Madden, P. A. *J. Chem. Phys.* **2004**, *121*, 7293.
(13) Aguado, A.; Bernasconi, L.; Jahn, S.; Madden, P. A. *Faraday Discuss.* **2003**, *124*, 171.

(14) Aguado, A.; Madden, P. A. *Phys. Rev. B* **2004**, *70*, 245103.
(15) Rahman, A.; Fowler, R. H.; Narten, A. H. *J. Chem. Phys.* **1972**, *57*, 3010.
(16) Brawer, S. A.; Weber, M. J. *J. Chem. Phys.* **1981**, *75*, 3516, 3522.
(17) Hemmati, M.; Moynihan, C. T.; Angell, C. A. *J. Chem. Phys.* **2001**, *115*, 6663.
(18) Madden, P. A.; Wilson, M. *J. Phys.: Condens. Matt.* **2000**, *12*, A95.
(19) Madden, P. A.; Heaton, R. J.; Aguado, A.; Jahn, S. *J. Mol. Struct. (THEOCHEM)*, to be published.
(20) Segall, M. D.; Lindan, P. J. D.; Probert, M. J.; Pickard, C. J.; Hasnip, P. J.; Clark, S. J.; Payne, M. C. *J. Phys.: Condens. Matt.* **2002**, *14*, 2717.
(21) Perdew, J. P. *Phys. Rev. B* **1992**, *45*, 13244.
(22) Rowley, A. J.; Jemmer, P.; Wilson, M.; Madden, P. A. *J. Chem. Phys.* **1998**, *108*, 10209.
(23) Becke, A. D.; Johnson, E. R. *J. Chem. Phys.* **2005**, *123*, 154101 and references therein.
(24) Dent, A.; Madden, P. A.; Wilson, M. *Solid State Ionics* **2004**, *167*, 73.
(25) Aguado, A.; Madden, P. A. *J. Chem. Phys.* **2003**, *119*, 7471.
(26) Vaslow, F.; Narten, A. H. *J. Chem. Phys.* **1973**, *59*, 4949.
(27) *International Tables for X-ray Crystallography*; Wilson, A. J. C., Ed.; Kluwer: Dordrecht, The Netherlands, 1992.
(28) Saika-Voivod, I.; Sciortino, F.; Poole, P. H. *Philos. Mag.* **2004**, *84*, 1437; *Nature* **2001**, *412*, 6846.
(29) Boulard, B.; Kieffer, J.; Phifer, C. C.; Angell, C. A. *J. Non-Cryst. Solids* **1992**, *140*, 350.
(30) Caillol, J. M.; Levesque, D.; Weiss, J.-J. *J. Chem. Phys.* **1989**, *91*, 5544, 5555.
(31) Gray-Weale, A.; Madden, P. A.; Wilson, M. *J. Chem. Phys.* **2000**, *113*, 6782.
(32) Wilson, M.; Madden, P. A.; Hemmati, M.; Angell, C. A. *Phys. Rev. Lett.* **1996**, *77*, 4023.
(33) Galeener, F. L.; Leadbetter, A. J.; Stringfellow, M. W. *Phys. Rev. B* **1983**, *27*, 1052.
(34) Tang, K. T.; Toennies, J. P. *J. Chem. Phys.* **1984**, *80*, 3726.